



Original article

Synthesis and biological evaluation of new *N*-alkyl 1-aryl-5-(1*H*-pyrrol-1-yl)-1*H*-pyrazole-3-carboxamides as cannabinoid receptor ligands

Romano Silvestri^{a,*}, Alessia Ligresti^b, Giuseppe La Regina^a, Francesco Piscitelli^{a,1}, Valerio Gatti^a, Antonio Lavecchia^{c,**}, Antonella Brizzi^d, Serena Pasquini^d, Marco Allarà^b, Noemi Fantini^e, Mauro Antonio Maria Carai^e, Chiara Bigogno^f, Marco Giulio Rozio^f, Roberta Sinisi^f, Ettore Novellino^c, Giancarlo Colombo^e, Vincenzo Di Marzo^b, Giulio Dondio^f, Federico Corelli^{d,***}

^aIstituto Pasteur – Fondazione Cenci Bolognietti, Dipartimento di Chimica e Tecnologie del Farmaco, Sapienza Università di Roma, Piazzale Aldo Moro 5, I-00185 Roma, Italy

^bIstituto di Chimica Biomolecolare, Consiglio Nazionale delle Ricerche, Via Campi Flegrei 34, Comprensorio Olivetti, I-80078 Pozzuoli, Napoli, Italy

^cUniversità di Napoli Federico II, Via Domenico Montesano 49, I-80131 Napoli, Italy

^dDipartimento Farmaco Chimico Tecnologico, Università di Siena, Polo Scientifico Universitario San Miniato, Via Alcide De Gasperi 2, I-53100 Siena, Italy

^eIstituto di Neuroscienze, Consiglio Nazionale delle Ricerche, Viale Armando Diaz 182, I-09126 Cagliari, Italy

^fNiKem Research Srl, Via Zambelletti 25, 20021 Baranzate, Milano, Italy

ARTICLE INFO

Article history:

Received 11 June 2010

Received in revised form

20 September 2010

Accepted 21 September 2010

Available online 1 October 2010

Keywords:

Cannabinoid

Human recombinant CB receptor type 1

Pyrrrole bioisoteres

Structure-activity relationships

Pharmacological studies

ABSTRACT

A series of *N*-alkyl 1-aryl-5-(1*H*-pyrrol-1-yl)-1*H*-pyrazole-3-carboxamides were synthesized as new ligands of the human recombinant receptor hCB₁. *n*-Alkyl carboxamides brought out different SARs from the branched subgroup. Unsubstituted pyrrole derivatives bearing a *tert*-alkyl chain at the 3-carboxamide nitrogen showed greater hCB₁ receptor affinity than the corresponding unbranched compounds. In particular, the *tert*-butyl group as a chain terminal moiety strongly improved hCB₁ receptor affinity (compound **24**: $K_i = 45.6$ nM; **29**: $K_i = 37.5$ nM). Acute administration of either compound **12** or **29** resulted in a specific, dose-dependent reduction in food intake in rats. Such results provide a useful basis for the design of new CB₁ ligands.

© 2010 Elsevier Masson SAS. All rights reserved.

1. Introduction

Obesity is a predisposing factor for the development of type-2 diabetes, hypertension, and cardiovascular disease [1]. Therapeutic options for morbidly obese patients are limited, as currently only two drugs have been approved by FDA in the United States for the long-term treatment of obesity, that is, sibutramine and orlistat. However, such agents provide modest reduction of the body weight, and both drugs are associated with adverse effects that have restricted their therapeutic potential [2]. Alternative treatments are thus desirable [3].

The endocannabinoid system is involved in various pathological conditions, such as pain, immunosuppression, peripheral vascular disease, appetite enhancement/suppression, and locomotor disorders [4]. In 2006, Sanofi–Aventis launched Rimobant (SR141716, **1**, Fig. 1) in the European Union as a CB₁ receptor inverse agonist for the treatment of overweight and obesity, and associated cardiovascular and metabolic disorders. In 2008, **1** was withdrawn from all other markets due to gastrointestinal side effects, depression and anxiety. Despite **1**'s failure, many research groups from academia and industry are still actively searching for novel CB₁ receptor antagonists [5], that may provide options for the treatment of obesity, whose prevalence is rapidly increasing globally, and has reached epidemic proportions in the developed countries. For example, Taranabant (**2**), Otenabant (**3**) Ibipinabant (**4**) and AVE1625 (**5**) are new CB₁ receptor antagonists/inverse agonists which have also been evaluated in clinical studies (**2** and **3** have been recently suspended from clinical development since they showed unwanted effects similar to **1**) [6].

* Corresponding author. Tel.: +39 06 4991 3800; fax: +39 06 4969 3268.

** Corresponding author. Tel./fax: +39 081 678 613.

*** Corresponding author. Tel.: +39 0577 234308; fax: +39 0577 234299.

E-mail addresses: romano.silvestri@uniroma1.it (R. Silvestri), lavecchi@unina.it (A. Lavecchia), corelli@unisi.it (F. Corelli).

¹ Present address: University of Pennsylvania, Department of Chemistry, 231 South 34th Street, Philadelphia, PA 19104-6323, USA.

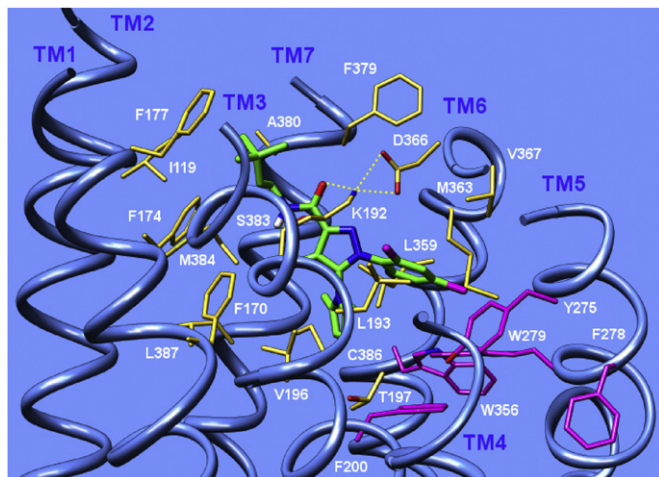


Fig. 1. View from the plane of the cell membrane of the **29**/hCB₁ complex. Only amino acids located within 4 Å distance from the ligand (green) are shown in yellow and labeled. Residues that form part of the aromatic cluster complex with the ligand are colored in magenta. H-bonds are indicated by dashed yellow lines. (For interpretation of the references to colour in this figure legend, the reader is referred to the web version of this article).

In search for new CB₁ receptor antagonists/inverse agonists, several chemical modifications of the template of **1** have been explored. Mainly, three diverse structural strategies resulted in the synthesis of: (i) pyrazole analogues of **1**, for example AM251 (**6**), (ii) bioisosteric compounds containing different heterocyclic rings in place of the pyrazole nucleus [7], and (iii) compounds representing structural simplification/complication of **1**'s template [8] (Chart 1).

Replacement of the 4-chlorophenyl group at position 5 of **1** with a pyrrole nucleus led us to disclose a new class of potent and selective CB₁ inverse agonists [9]. Structural modification of these prototypical compounds led to new ligands endowed with affinity and selectivity for the human CB₁ (hCB₁) receptor comparable to the reference compounds **1** and **6**. In particular, derivatives bearing

an aliphatic substituent at the 3-carboxamide nitrogen showed the highest affinity for the CB₁ receptor, e.g. **7** [$K_i(\text{CB}_1) = 3.4 \text{ nM}$] [10].

Such findings prompted us to synthesize new carboxamide derivatives bearing selected aliphatic chains at the nitrogen atom. Herein, we describe the synthesis and the biological evaluation of both linear carboxamides **8–20** and isomeric branched carboxamides **21–31** (Fig. 1, Table 1).

2. Chemistry

Synthesis of carboxamides **8–31** was performed by coupling reactions of previously described acids **32–35** [10] with either unbranched or branched aliphatic amines in the presence of *N*-ethyl-*N'*-(3-dimethylaminopropyl)carbodiimide (EDC) hydrochloride and 1-hydroxybenzotriazole (HOBt). Morpholinomethyl polystyrene and polymer bound *para*-toluenesulfonic acid were used as scavengers for acidic and basic substances, respectively (Scheme 1).

3. Results and discussion

3.1. Binding affinity

The binding affinities (K_i values) of **8–31** for the human recombinant CB receptors hCB₁ and hCB₂ were evaluated in parallel with reference compounds **1–3** (Table 1). The binding to the receptor was evaluated by means of membranes from HEK cells transfected with either the hCB₁ or hCB₂ receptor and [³H]-CP-55,940. The high affinity ligand K_d values were 0.18 nM for CB₁ receptor, and 0.31 nM for CB₂ receptor [11]. Displacement curves were derived after incubation of the drugs with [³H]-CP-55,940 at 0.14 nM for CB₁ and 0.084 nM for CB₂ binding assay. The K_i values were calculated from the IC₅₀ values according to the Cheng–Prusoff equation [12].

We first synthesized carboxamides **8–20** bearing C3–C7 normal alkyl chains at the 3-carboxamide nitrogen. Compounds **8–20** showed affinity for the hCB₁ receptor with K_i values ranging from 81.0 (**10**) to 550.3 (**8**) nM (Table 1). Compound **17** (CB₁ SI = 8.6; CB₁ selectivity index (SI) was calculated as $K_i(\text{CB}_2)/K_i(\text{CB}_1)$ ratio) had the

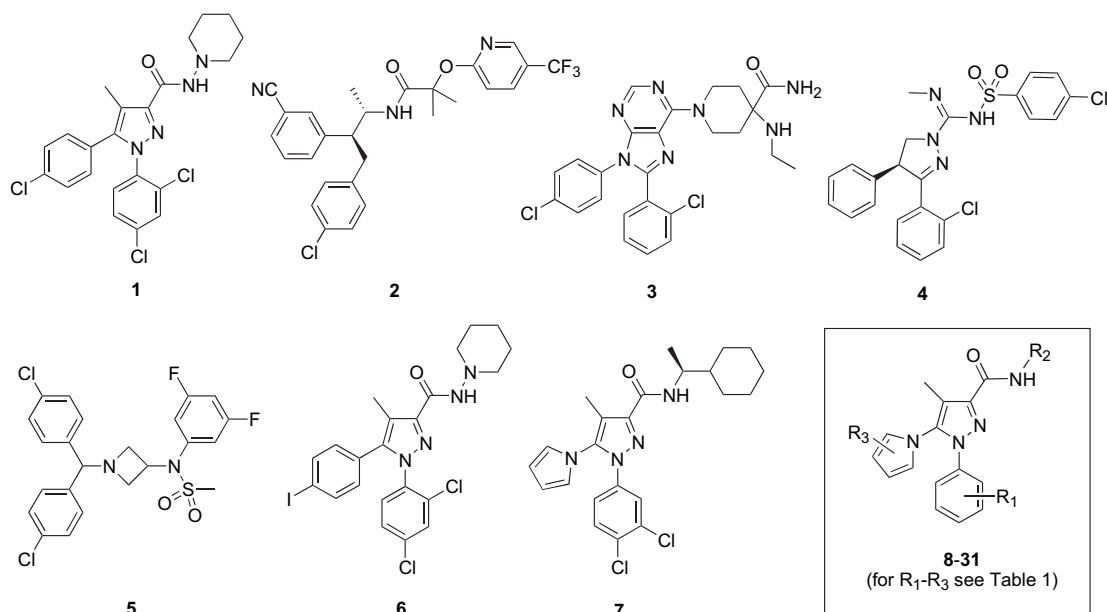
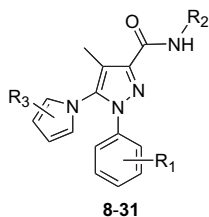


Chart 1. Structures of reference compounds **1–7** and new compounds **8–31**.

Table 1
Structure, hCB₁ and hCB₂ receptor affinity (³H]CP-55,940 radioligand) of carboxamides **8–31**.^a



Compd.	R ₁	R ₂	R ₃	K _i (nM) ^b		
				hCB ₁	hCB ₂	SI ^c
8	2,4-Cl ₂		H	550.3	1496.2	2.71
9	2,4-Cl ₂		H	272.6	795.7	2.91
10	2,4-Cl ₂		H	81.0	205.9	2.54
11	2,4-Cl ₂		H	534.4	2344.4	4.38
12	2,4-Cl ₂		H	124.1	383.3	3.09
13	2,4-Cl ₂		H	211.0	255.1	1.21
14	2,4-Cl ₂		2,5-Me ₂	290.1	1953.3	6.73
15	2,4-Cl ₂		2,5-Me ₂	123.1	459.8	3.73
16	2,4-Cl ₂		2,5-Me ₂	182.1	495.3	2.72
17	2,4-Cl ₂		2,5-Me ₂	372.3	3200.5	8.59
18	2,4-F ₂		2,5-Me ₂	311.4	487.3	1.56
19	2,4-Cl ₂		2,5-Me ₂	97.2	204.8	2.11
20	2,4-F ₂		2,5-Me ₂	368.2	365.5	0.99
21	2,4-Cl ₂		H	518.9	1132.4	2.18
22	2,4-Cl ₂		H	89.5	14.6	0.16
23	2,4-Cl ₂		H	47.6	5.70	0.11

Table 1 (continued)

Compd.	R ₁	R ₂	R ₃	K _i (nM) ^b		
				hCB ₁	hCB ₂	SI ^c
24	2,4-Cl ₂		H	45.6	52.4	1.15
25	2,4-Cl ₂		H	157.5	237.3	1.51
26	2,4-Cl ₂		2,5-Me ₂	233.5	1796.8	7.69
27	2,4-Cl ₂		2,5-Me ₂	150.7	20.2	0.13
28	2,4-Cl ₂		2,5-Me ₂	193.5	121.5	0.62
29	2,4-Cl ₂		2,5-Me ₂	37.5	133.5	3.56
30	2,4-Cl ₂		2,5-Me ₂	104.7	135.5	1.29
31	2,4-F ₂		2,5-Me ₂	90.7	163.4	1.80
RI ^d	—	—	—	12	790	65.83
AM ^e	—	—	—	2.3	112	48.70
SR ^f	—	—	—	>2820	5.4	<0.002

^a Data represent mean values for at least three separate experiments performed in duplicate. Standard error of means (SEM) are not shown for the sake of clarity and were never higher than 5% of the means.

^b K_i and IC₅₀ are defined in experimental section.

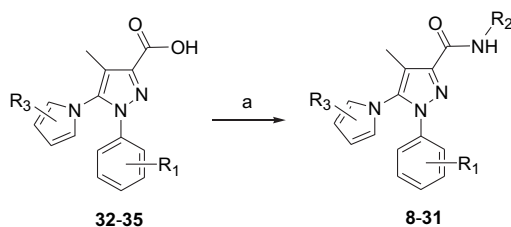
^c SI: CB₁ selectivity index was calculated as K_i(CB₂)/K_i(CB₁) ratio.

^d RI: Rimonabant (**1**), CB₁ reference compound.

^e AM: AM251 (**6**), CB₁ reference compound.

^f SR: SR144528, CB₂ reference compound.

highest CB₁ SI value, and derivatives **10** and **19** showed K_i values <100 nM. Introduction of a hydroxy group at ω position of the n-pentyl chain of either **10** or **16** provided more selective CB₁



32: R₁ = 2,4-Cl₂, R₃ = H; **33**: R₁ = 2,4-Cl₂, R₃ = 2,5-Me₂;
34: R₁ = 2,4-F₂, R₃ = H; **35**: R₁ = 2,4-F₂, R₃ = 2,5-Me₂;
8-31: for R₁-R₃ substituents, see Table 1.

Scheme 1. Synthesis of carboxamides **8–31**. Reagents and conditions. a: (i) R₂NH₂, HOBT, EDC, dichloromethane, 0 °C to room temp., overnight; (ii) morpholinomethyl polystyrene and polymer bound *p*-toluenesulfonic acid, room temp., 24 h; yield 48–98%.

ligands (**11**: CB₁ SI = 4.4, and **17**: CB₁ SI = 8.6) as a result of reduced affinity for the hCB₂ receptor. The CB₁ receptor affinity of carboxamides **8–20** was not dramatically affected by the length of the *n*-alkyl chain, even in the presence of methyl groups at position 2 and 5 of the pyrrole ring (compare **9** with **12** and **13**, and **15** with **16** and **19**).

In preliminary pharmacokinetic studies in the rat, carboxamide **12** was quickly available in plasma and brain (T_{\max} = 30 min) after i.p. administration at 10 mg/kg. The concentration of compound **12** in the two compartments was very similar over time (C_{\max} 170 ng/mL and 110 ng/g in plasma and brain, respectively). $T_{1/2}$ calculated on the elimination phase and MRT were very similar in plasma and brain (about 850 min). The brain penetration calculated as a ratio of the AUCs was about 97% (Table 2).

Introduction of branched alkyl chains at the 3-carboxamide nitrogen led to derivatives **21–31** which were endowed with higher receptor affinity for both CB₁ and CB₂ subtypes. The improvement of affinity was particularly correlated to the presence of a *tert*-butyl moiety. On the other hand, the CB receptor affinity was also greatly affected by the substitution pattern at position 5 of the pyrrole nucleus. Derivatives bearing both unsubstituted pyrrole nucleus and *tert*-alkyl chain at the amide nitrogen, generally showed greater hCB₁ receptor affinity than the corresponding unbranched compounds. Such a chemical modification also resulted in significant improvement of affinity for the hCB₂ receptor of **22**, **23** and **24** (compare **22** with **9** (C4), **23** with **10** (C5) and **24** with **12** (C6)). The *tert*-butyl moiety strongly affected the receptor affinity when it was placed as a chain terminator group (**24**, **29** and **31**). Accordingly, compounds **24** (K_i = 45.6 nM) and **29** (K_i = 37.5 nM) showed the highest affinity for the hCB₁ receptor.

3.2. Molecular modeling

The H-bond with K3.28(192) is recognized to be crucial for the high affinity of **1** to the inactive receptor state and its inverse agonism activity, by stabilizing a salt bridge between K3.28(192) and D6.58(366) [13]. In MD experiments using our previously published homology model of the inactive state of hCB₁ [9,10], the carboxamide oxygen of **29** formed an H-bond with K3.28(192) during the whole simulation time (Fig. 1). The *N*-*tert*-butyl group fitted into a pocket formed by the lipophilic residues I1.34(119), F2.57(170), F2.61(174), F2.64(177), and A7.36(380). The 2,5-dimethylpyrrole ring formed contacts with the hydrophobic residues V3.32(196) and C7.42(386), and projected the two methyl groups close to the lipophilic residues L6.51(359) and W5.43(279). The 4-methyl group formed hydrophobic interactions with V3.32(196) and F2.57(170) residues. Finally, the 2,4-dichlorophenyl ring at position 1 of the pyrazole nucleus was embedded within a hydrophobic pocket formed by L3.29(193), Y5.39(275), W5.43(279), L6.51(359), M6.55

(363), and V6.59(367), and established favourable π - π stacking interactions with the indole ring of W5.43(279). Such interactions involved the aromatic residue-rich TM3-4-5-6 region of hCB₁ [14] (in magenta), and were stable during the MD trajectory (the electron-withdrawing chlorine atoms contribute to strengthening the stacking interactions). **29** showed typical binding interactions previously reported for this class of CB₁ ligands [9,10].

3.3. Pharmacological studies

The effects on reduction in food intake were evaluated in rats after administration of either compound **12** or **29**. ANOVA revealed significant effects of treatment with either compound **12** [$F_{(3,28)} = 8.47$, $P < 0.0005$] or **29** [$F_{(2,20)} = 7.62$, $P < 0.005$] on cumulative food intake over the first 6 h after lights off. Post hoc analysis (Mann–Whitney test) revealed significant differences ($P < 0.05$) between the rat group treated with vehicle and (a) the rat group treated with **12** (1 mg/kg) or **29** (3 mg/kg) at the 2-, 3-, 4-, 5-, and 6-h time intervals and (b) the rat group treated with 10 mg/kg **12** or **29** at all six time intervals (**12**: Fig. 2, top panel; **29**: Fig. 3, top panel). Magnitude of reduction, with respect to vehicle-treated rats, averaged 10–30% and 25–35% in the rat groups treated with 1 and 10 mg/kg **12**, respectively. Conversely, the 0.1-mg/kg dose of **12** was virtually ineffective in altering food intake at each time interval.

At the 24-h time interval, no difference in food intake was recorded between rats treated with both doses of compound **12** and rats treated with vehicle [$F_{(3,28)} = 2.29$, $P > 0.05$] (Fig. 2, top panel). Magnitude of reduction, with respect to vehicle-treated rats, averaged 10–35% and 30–40% in the rat groups treated with 3 and 10 mg/kg **29**, respectively (Fig. 3, top panel).

The reducing effect of **29** on food intake was still evident at the 24-h time interval [$F_{(2,20)} = 5.88$, $P < 0.05$] (Fig. 3, top panel). Post hoc analysis indicated that food intake in 3 and 10 mg/kg-treated rat groups was significantly ($P < 0.05$) lower than in the vehicle-treated rat group. Reduction in food intake disappeared in the following 2 days (data not shown). The reducing effect of **12** or **29** was specific for food intake, as such compounds did not affect cumulative water intake over the first 6 h after lights off [**12**: $F_{(3,28)} = 2.47$, $P > 0.05$;

Table 2

Rat pharmacokinetic parameters of **12** (10 mg/kg, ip).

Parameter	Plasma	Brain
C_{\max}^a (ng/mL or ng/g) ^b	170 ± 61	110 ± 13
T_{\max}^c (min)	30	30
$T_{1/2}^d$ (min)	836	862
MRT_{inf}^e (min)	889	860
AUC_{last}^f (min ng/mL)	20414	19801
Brain penetration (%)	–	97

^a C_{\max} : maximum concentration.

^b Data represent mean values of three rats ± S.D.

^c T_{\max} : time when the maximum concentration is reached.

^d $T_{1/2}$: half life.

^e MRT_{inf} : mean residence time calculated at the infinity.

^f AUC_{last} : area under the curve calculated up to the last timepoint.

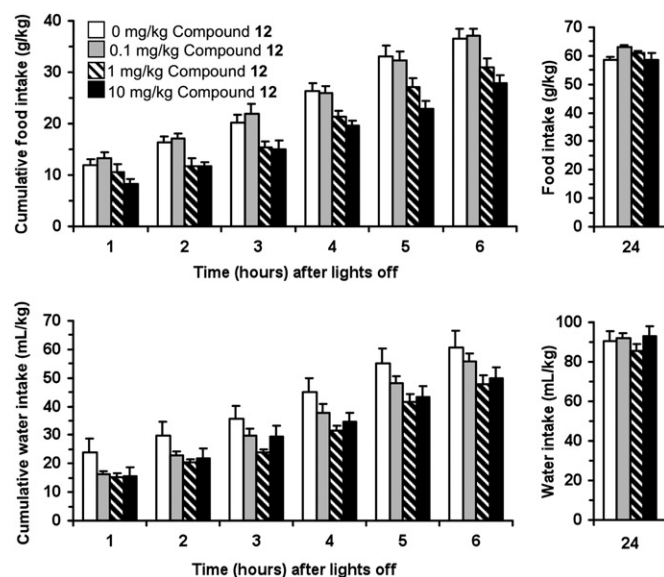


Fig. 2. Effect of the acute administration of different doses of compound **12** on food (top panel) and water (bottom panel) intake in Wistar rats given unlimited access to regular rodent chow and water. Each bar is the mean ± SEM of $n = 8$ rats.

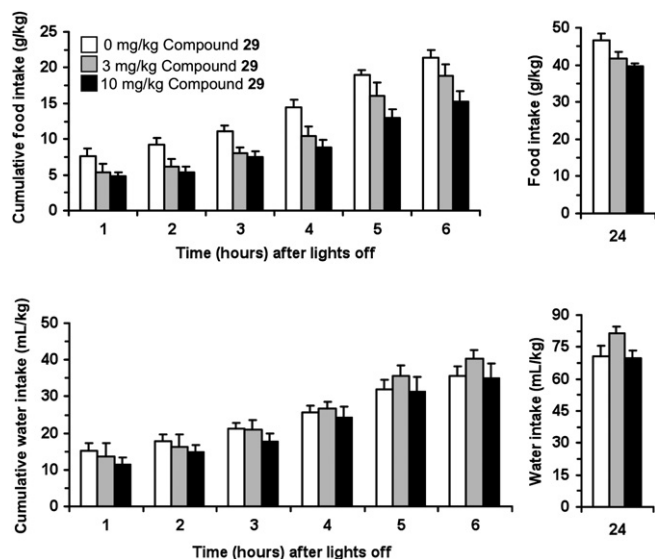


Fig. 3. Effect of the acute administration of different doses of compound **29** on food (top panel) and water (bottom panel) intake in Wistar rats given unlimited access to regular rodent chow and water. Each bar is the mean \pm SEM of $n = 7$ –8 rats.

29: $F_t(2,20) = 0.44, P > 0.05$] as well as water intake at the 124-h time interval [**12:** $F(3,28) = 0.63, P > 0.05$], Fig. 2, bottom panel; [**29:** $F(2,20) = 2.38, P > 0.05$], Fig. 3, bottom panel.

Compounds **12** at 1 and 10 mg/kg and **29** at 3 and 10 mg/kg reduced food intake in rats, and revealed comparable potency and efficacy. However, the reducing effect of **29** on food intake seemed to be longer-lasting than that of **12**, as reduction in food intake was still evident 24 h after drug injection. Although caution has to be used when comparing data from different sets of experiments, compounds **12** and **29** seemed to be slightly less effective in reducing food intake in rats than **1** [15]. The *in vivo* anorectic effect of **12** and **29** may be correlated to their antagonist/inverse agonist activity at the cannabinoid CB₁ receptor [15,16] Such a hypothesis needs to be confirmed by additional evidences.

4. Conclusion

We have synthesized new *N*-alkyl 1-aryl-5-(1*H*-pyrrol-1-yl)-1*H*-pyrazole-3-carboxamides as human recombinant receptor hCB₁ ligands. SARs of *n*-alkyl (**8**–**20**) and branched (**21**–**31**) carboxamide subgroups highlighted different rules. The CB₁ receptor affinity of carboxamides **8**–**20** was not dramatically affected by the length of the C3–C7 *n*-alkyl chain, even in the presence of methyl groups at position 2 and 5 of the pyrrole ring. In pharmacokinetic studies, compound **12** reached significant plasma and brain concentrations, and supported its centrally mediated anorectic effect after acute administration in the rat. Unsubstituted pyrrole derivatives bearing a *tert*-alkyl chain at the amide nitrogen showed greater hCB₁ receptor affinity than the corresponding unbranched compounds. In particular, the *tert*-butyl moiety as a chain terminal group, effectively improved the hCB₁ receptor affinity (**24:** $K_i = 45.6$ nM; **29:** $K_i = 37.5$ nM). In MD simulations, the carboxamide oxygen of **29** formed an H-bond with K3.28(192) during the whole simulation time, as it did for **1**. Acute administration of **12** and **29** resulted in a specific, dose-dependent reduction in food intake in rats; **12** at 1 and 10 mg/kg and **29** at 3 and 10 mg/kg showed comparable potency and effectiveness. On food intake, however, **29** exhibited longer-lasting reducing effect, as reduction in food intake was still evident 24 h after drug injection. The results described here provide a useful basis for the design of new hCB₁ ligands.

5. Experimental protocols

5.1. Chemistry

Melting points (mp) were determined on a Büchi 510 apparatus and are uncorrected. Infrared spectra (IR) were run on a Spectrum One spectrophotometer. Band position and absorption ranges are given in cm^{-1} . Proton nuclear magnetic resonance (¹H NMR) spectra were recorded on a Bruker Avance 400 MHz FT spectrometer in the indicated solvent. Chemical shifts are expressed in δ units (ppm) from tetramethylsilane. Chromatography columns were packed with Merck silica gel (70–230 mesh). Aluminum oxide TLC cards from Fluka (aluminum oxide precoated aluminum cards with fluorescent indicator at 254 nm) and silica gel TLC cards from Fluka (silica gel precoated aluminum cards with fluorescent indicator at 254 nm) were used for thin layer chromatography (TLC). Developed plates were visualized with a Spectroline ENF 260C/F UV apparatus. Organic solutions were dried over anhydrous sodium sulfate. Concentration and evaporation of the solvents was carried out on a Büchi Rotavapor R-210 equipped with a Büchi V-850 vacuum controller and Büchi V-700 (approx. 5 mbar) and V-710 vacuum (approx. 2 mbar) pumps. Compound purity was determined by combustion analysis. Elemental analyses were within $\pm 0.4\%$ of the theoretical values. Purity of tested compounds was $>95\%$. Büchi Syncore reactor was used for parallel synthesis, filtration, and evaporation.

5.1.1. Parallel synthesis of amides **8**–**31**

EDC hydrochloride (1.2 mmol) and HOBt (1.0 mmol) were added at 0 °C to each parallel vial containing a solution of the appropriate acid **32**–**35** [10] (1 mmol) in dichloromethane, and the selected amines (1.5 mmol) were added at the same temperature. After warm up to room temperature, the vials were placed in the Büchi Syncore reactor. Stirring was maintained at 300 rpm overnight and then morpholinomethyl polystyrene (3 eq/mol) was added. The solutions were kept at room temperature for 1 h, then polymer bound *p*-toluenesulfonic acid (3 eq/mol) was added to each vial, and the reaction mixtures were stirred at room temperature for an additional 24 h. The mixtures were filtered and the solutions were evaporated to dryness to give carboxamides **8**–**31**. Solid products were purified by crystallization from ethanol or aqueous ethanol (**18** and **30**). Oil products were purified by silica gel chromatography column (dichloromethane as eluent).

5.1.1.1. 1-(2,4-Dichlorophenyl)-4-methyl-*N*-propyl-5-(1*H*-pyrrol-1-yl)-1*H*-pyrazole-3-carboxamide (8**).** Yield 98% as a white solid, mp 125–127 °C (from ethanol). ¹H NMR (CDCl₃): δ 0.99 (t, $J = 7.4$ Hz, 3H), 1.64 (sx, $J = 7.3$ Hz, 2H), 2.32 (s, 3H), 3.40 (q, $J = 6.8$ Hz, 2H), 6.20–6.21 (m, 2H), 6.58–6.59 (m, 2H), 6.98 (broad s, 1H, disappeared on treatment with D₂O), 7.22 (d, $J = 8.2$ Hz, 1H), 7.29 (dd, $J = 8.5$ and 2.2 Hz, 1H), 7.49 ppm (d, $J = 2.2$ Hz, 1H). IR: ν 1653, 3413 cm^{-1} . Anal. Calcd. for C₁₈H₁₈Cl₂N₄O: C, 57.30%; H, 4.81%; N, 14.85%. Found: C, 57.19%; H, 4.78%; N, 14.74%.

5.1.1.2. *N*-Butyl-1-(2,4-dichlorophenyl)-4-methyl-5-(1*H*-pyrrol-1-yl)-1*H*-pyrazole-3-carboxamide (9**).** Yield 98% as a white solid, mp 121–122 °C (from ethanol). ¹H NMR (CDCl₃): δ 0.96 (t, $J = 7.3$ Hz, 3H), 1.42 (sx, $J = 7.7$ Hz, 2H), 1.60 (qn, $J = 7.5$ Hz, 2H), 2.32 (s, 3H), 3.44 (q, $J = 6.8$ Hz, 2H), 6.21–6.22 (m, 2H), 6.58–6.59 (m, 2H), 6.94 (broad s, 1H, disappeared on treatment with D₂O), 7.22 (d, $J = 8.5$ Hz, 1H), 7.29 (dd, $J = 8.5$ and 2.2 Hz, 1H), 7.48 ppm (d, $J = 2.2$ Hz, 1H). IR: ν 1655, 3428, cm^{-1} . Anal. Calcd. for C₁₉H₂₀Cl₂N₄O: C, 58.32%; H, 5.15%; N, 14.32%. Found: C, 58.11%; H, 5.11%; N, 14.16%.

5.1.1.3. 1-(2,4-Dichlorophenyl)-4-methyl-N-pentyl-5-(1H-pyrrol-1-yl)-1H-pyrazole-3-carboxamide (**10**). Yield 91% as a white solid, mp 79–80 °C (from ethanol). ¹H NMR (CDCl₃): δ 0.93 (t, *J* = 7.1 Hz, 3H), 1.33–1.39 (m, 4H), 1.59–1.61 (m, 2H), 2.32 (s, 3H), 3.43 (q, *J* = 6.9 Hz, 2H), 6.20–6.21 (m, 2H), 6.58–6.59 (m, 2H), 6.95 (broad s, 1H, disappeared on treatment with D₂O), 7.22 (d, *J* = 8.5 Hz, 1H), 7.29 (dd, *J* = 8.5 and 2.2 Hz, 1H), 7.48 ppm (d, *J* = 2.2 Hz, 1H). IR: ν 1666, 3420 cm⁻¹. Anal. Calcd. for C₂₀H₂₂Cl₂N₄O: C, 59.27%; H, 5.47%; N, 13.82%. Found: C, 59.08%; H, 5.41%; N, 13.73%.

5.1.1.4. 1-(2,4-Dichlorophenyl)-N-(5-hydroxypentyl)-4-methyl-5-(1H-pyrrol-1-yl)-1H-pyrazole-3-carboxamide (**11**). Yield 98% as a colorless oil. ¹H NMR (CDCl₃): δ 1.37 (broad s, 1H, disappeared on treatment with D₂O), 1.46–1.51 (m, 2H), 1.60–1.68 (m, 4H), 2.31 (s, 3H), 3.45 (q, *J* = 6.7 Hz, 2H), 3.67 (t, *J* = 6.5 Hz, 2H), 6.21–6.22 (m, 2H), 6.57–6.58 (m, 2H), 6.99 (broad s, 1H, disappeared on treatment with D₂O), 7.22 (d, *J* = 8.4 Hz, 1H), 7.29 (dd, *J* = 8.4 and 2.2 Hz, 1H), 7.49 ppm (d, *J* = 1.9 Hz, 1H). IR: ν 1656, 3410 cm⁻¹. Anal. Calcd. for C₂₀H₂₂Cl₂N₄O₂: C, 57.01%; H, 5.26%; N, 13.30%. Found: C, 56.79%; H, 5.21%; N, 13.19%.

5.1.1.5. 1-(2,4-Dichlorophenyl)-N-hexyl-4-methyl-5-(1H-pyrrol-1-yl)-1H-pyrazole-3-carboxamide (**12**). Yield 70% as a colorless oil. ¹H NMR (200 MHz, CDCl₃): δ 0.80 (t, *J* = 6.0 Hz, 3H), 1.24–1.40 (m, 6H), 1.47–1.54 (m, 2H), 2.22 (s, 3H), 3.27–3.37 (m, 2H), 6.10 (s, 2H), 6.50 (s, 2H), 6.90–6.99 (m, 2H), 7.19 (s, 1H), 7.39 (s, 1H). MS (ESI): *m/z*: 420 [M + H]⁺. IR (CHCl₃): ν 1653 cm⁻¹. Anal. Calcd. for C₂₁H₂₄Cl₂N₄O: C, 60.15%; H, 5.77%; N, 13.36%. Found: C, 59.88%; H, 5.54%; N, 13.17%.

5.1.1.6. 1-(2,4-Dichlorophenyl)-N-heptyl-4-methyl-5-(1H-pyrrol-1-yl)-1H-pyrazole-3-carboxamide (**13**). Yield 97% as a colorless oil. ¹H NMR (CDCl₃): δ 0.89 (t, *J* = 6.7 Hz, 3H), 1.29–1.38 (m, 8H), 1.61 (qn, *J* = 7.3 Hz, 2H), 2.31 (s, 3H), 3.42 (q, *J* = 6.7 Hz, 2H), 6.20–6.21 (m, 2H), 6.58–6.59 (m, 2H), 6.95 (broad s, 1H, disappeared on treatment with D₂O), 7.22 (d, *J* = 8.5 Hz, 1H), 7.29 (dd, *J* = 8.5 and 2.2 Hz, 1H), 7.48 ppm (d, *J* = 2.2 Hz, 1H). IR: ν 1668, 3419 cm⁻¹. Anal. Calcd. for C₂₂H₂₆Cl₂N₄O: C, 60.97%; H, 6.05%; N, 12.93%. Found: C, 60.77%; H, 6.03%; N, 12.83%.

5.1.1.7. 1-(2,4-Dichlorophenyl)-5-(2,5-dimethyl-1H-pyrrol-1-yl)-4-methyl-N-propyl-1H-pyrazole-3-carboxamide (**14**). Yield 71% as a white solid, mp 84–86 °C (from ethanol). ¹H NMR (CDCl₃): δ 1.01 (t, *J* = 7.4 Hz, 3H), 1.67 (qn, *J* = 7.3 Hz, 2H), 1.96 (s, 6H), 2.20 (s, 3H), 3.42 (q, *J* = 7.0 Hz, 2H), 5.82 (s, 2H), 6.91 (d, *J* = 8.5 Hz, 1H), 7.05 (broad s, 1H, disappeared on treatment with D₂O), 7.20 (dd, *J* = 8.5 and 2.9 Hz, 1H), 7.53 ppm (d, *J* = 2.3 Hz, 1H). IR: ν 1654, 3330 cm⁻¹. Anal. Calcd. for C₂₀H₂₂Cl₂N₄O: C, 59.27%; H, 5.47%; N, 13.82%. Found: C, 59.06%; H, 5.40%; N, 13.72%.

5.1.1.8. N-Butyl-1-(2,4-dichlorophenyl)-5-(2,5-dimethyl-1H-pyrrol-1-yl)-4-methyl-1H-pyrazole-3-carboxamide (**15**). Yield 98% as a white solid, mp 67–69 °C (from ethanol). ¹H NMR (CDCl₃): δ 0.97 (t, *J* = 7.3 Hz, 3H), 1.44 (sx, *J* = 7.7 Hz, 2H), 1.61 (qn, *J* = 7.8 Hz, 2H), 1.96 (s, 6H), 2.20 (s, 3H), 3.46 (q, *J* = 6.6 Hz, 2H), 5.81 (s, 2H), 6.91 (d, *J* = 8.5 Hz, 1H), 7.01 (broad s, 1H, disappeared on treatment with D₂O), 7.21 (dd, *J* = 8.5 and 2.3 Hz, 1H), 7.53 ppm (d, *J* = 2.2 Hz, 1H). IR: ν 1669, 3419 cm⁻¹. Anal. Calcd. for C₂₁H₂₄Cl₂N₄O: C, 60.15%; H, 5.77%; N, 13.36%. Found: C, 59.87%; H, 5.72%; N, 13.24%.

5.1.1.9. 1-(2,4-Dichlorophenyl)-5-(2,5-dimethyl-1H-pyrrol-1-yl)-4-methyl-N-pentyl-1H-pyrazole-3-carboxamide (**16**). Yield 71% as a white solid, mp 54–56 °C (from ethanol/water). ¹H NMR (CDCl₃): δ 0.92 (t, *J* = 7.1 Hz, 3H), 1.37–1.40 (m, 4H), 1.59–1.64 (m, 2H), 1.96 (s, 6H), 2.20 (s, 3H), 3.43 (q, *J* = 6.9 Hz, 2H), 5.82 (s, 2H), 6.91 (d, *J* = 8.6 Hz, 1H), 7.01 (broad s, 1H, disappeared on treatment with

D₂O), 7.20 (dd, *J* = 8.6 and 2.3 Hz, 1H), 7.53 ppm (d, *J* = 2.3 Hz, 1H). IR: ν 1669, 3415 cm⁻¹. Anal. Calcd. for C₂₂H₂₆Cl₂N₄O: C, 60.97%; H, 6.05%; N, 12.93%. Found: C, 60.71%; H, 6.00%; N, 12.81%.

5.1.1.10. 1-(2,4-Dichlorophenyl)-5-(2,5-dimethyl-1H-pyrrol-1-yl)-N-(5-hydroxypentyl)-4-methyl-1H-pyrazole-3-carboxamide (**17**). Yield 98% as a colorless oil. ¹H NMR (CDCl₃): δ 1.44 (broad s, 1H, disappeared on treatment with D₂O), 1.47–1.53 (m, 2H), 1.61–1.71 (m, 4H), 1.96 (s, 6H), 2.20 (s, 3H), 3.47 (q, *J* = 6.7 Hz, 2H), 3.68 (t, *J* = 6.0 Hz, 2H), 5.82 (s, 2H), 6.91 (d, *J* = 8.5 Hz, 1H), 7.06 (broad s, 1H, disappeared on treatment with D₂O), 7.21 (dd, *J* = 8.5 and 2.3 Hz, 1H), 7.53 ppm (d, *J* = 2.3 Hz, 1H). IR: ν 1657, 3412 cm⁻¹. Anal. Calcd. for C₂₂H₂₆Cl₂N₄O₂: C, 58.80%; H, 5.83%; N, 12.47%. Found: C, 58.63%; H, 5.78%; N, 12.38%.

5.1.1.11. 1-(2,4-Difluorophenyl)-5-(2,5-dimethyl-1H-pyrrol-1-yl)-N-hexyl-4-methyl-1H-pyrazole-3-carboxamide (**18**). Yield 77% as cream solid, mp 77–79 °C ¹H NMR (CDCl₃): δ 0.87 (t, 3H, *J* = 6.4 Hz), 1.44–1.23 (m, 6H), 1.64–1.53 (m, 2H), 1.88 (s, 6H), 2.16 (s, 3H), 3.46–3.36 (m, 2H), 5.78 (s, 2H), 7.06–6.83 (m, 2H), 7.17–7.09 ppm (m, 1H). MS *m/z*: 415 [M + 1]⁺ (20%), 437 [M + 23]⁺ (100%).

5.1.1.12. 1-(2,4-Dichlorophenyl)-5-(2,5-dimethyl-1H-pyrrol-1-yl)-N-heptyl-4-methyl-1H-pyrazole-3-carboxamide (**19**). Yield 75% as a white solid, mp 51–56 °C (from ethanol-water). ¹H NMR (CDCl₃): δ 0.89 (t, *J* = 6.9 Hz, 3H), 1.26–1.33 (m, 8H), 1.61 (qn, *J* = 7.3 Hz, 2H), 1.96 (s, 6H), 2.20 (s, 3H), 3.44 (q, *J* = 6.5 Hz, 2H), 5.82 (s, 2H), 6.90 (d, *J* = 8.6 Hz, 1H), 7.01 (broad s, 1H, disappeared on treatment with D₂O), 7.20 (dd, *J* = 8.6 and 2.3 Hz, 1H), 7.53 ppm (d, *J* = 2.0 Hz, 1H). IR: ν 1670, 3421 cm⁻¹. Anal. Calcd. for C₂₄H₃₀Cl₂N₄O: C, 62.47%; H, 6.55%; N, 12.14%. Found: C, 62.19%; H, 6.50%; N, 11.98%.

5.1.1.13. 1-(2,4-Difluorophenyl)-5-(2,5-dimethyl-1H-pyrrol-1-yl)-N-heptyl-4-methyl-1H-pyrazole-3-carboxamide (**20**). Yield 48% as a white solid, mp 143–145 °C (from ethanol). ¹H NMR (CDCl₃): δ 0.89 (t, *J* = 6.8 Hz, 3H), 1.29–1.38 (m, 8H), 1.64 (qn, *J* = 7.3 Hz, 2H), 1.92 (s, 6H), 2.20 (s, 3H), 3.44 (q, *J* = 6.2 Hz, 2H), 5.82 (s, 2H), 6.88–6.95 (m, 2H), 6.99 (broad s, 1H, disappeared on treatment with D₂O), 7.14–7.18 ppm (m, 1H). IR: ν 1645, 3335 cm⁻¹. Anal. Calcd. for C₂₄H₃₀F₂N₄O: C, 67.27%; H, 7.06%; N, 13.07%. Found: C, 67.02%; H, 6.95%; N, 12.79%.

5.1.1.14. 1-(2,4-Dichlorophenyl)-N-isopropyl-4-methyl-5-(1H-pyrrol-1-yl)-1H-pyrazole-3-carboxamide (**21**). Yield 97% as a white solid, mp 124–126 °C (from ethanol). ¹H NMR (CDCl₃): δ 1.27 (d, *J* = 6.6 Hz, 6H), 2.32 (s, 3H), 4.19–4.24 (m, 1H), 6.21–6.22 (m, 2H), 6.58–6.59 (m, 2H), 6.77 (broad s, 1H, disappeared on treatment with D₂O), 7.24 (d, *J* = 8.4 Hz, 1H), 7.30 (dd, *J* = 8.5 and 2.2 Hz, 1H), 7.48 ppm (d, *J* = 2.3 Hz, 1H). IR: ν 1672, 3394 cm⁻¹. Anal. Calcd. for C₁₈H₁₈Cl₂N₄O: C, 57.30%; H, 4.81%; N, 14.85%. Found: C, 57.23%; H, 4.76%; N, 14.71%.

5.1.1.15. N-tert-Butyl-1-(2,4-dichlorophenyl)-4-methyl-5-(1H-pyrrol-1-yl)-1H-pyrazole-3-carboxamide (**22**). Yield 91% as a white solid, mp 101–103 °C (from ethanol). ¹H NMR (CDCl₃): δ 1.49 (s, 9H), 2.30 (s, 3H), 6.19–6.21 (m, 2H), 6.57–6.58 (m, 2H), 6.82 (broad s, 1H, disappeared on treatment with D₂O), 7.23 (d, *J* = 8.8 Hz, 1H), 7.29 (dd, *J* = 8.5 and 2.2 Hz, 1H), 7.48 ppm (d, *J* = 1.9 Hz, 1H). IR: ν 1672, 3407 cm⁻¹. Anal. Calcd. for C₁₉H₂₀Cl₂N₄O: C, 58.32%; H, 5.15%; N, 14.32%. Found: C, 58.20%; H, 5.13%; N, 14.21%.

5.1.1.16. 1-(2,4-Dichlorophenyl)-4-methyl-N-tert-pentyl-5-(1H-pyrrol-1-yl)-1H-pyrazole-3-carboxamide (**23**). Yield 98% as a white solid, mp 114–116 °C (from ethanol). ¹H NMR (CDCl₃): δ 0.93 (t, *J* = 7.5 Hz, 3H), 1.43 (s, 6H), 1.85 (q, *J* = 7.5 Hz, 2H), 2.32 (s, 3H), 6.20–6.22 (m, 2H), 6.57–6.58 (m, 2H), 6.75 (broad s, 1H,

disappeared on treatment with D₂O), 7.23 (d, *J* = 8.5 Hz, 1H), 7.29 (dd, *J* = 8.5 and 2.2 Hz, 1H), 7.48 ppm (d, *J* = 2.2 Hz, 1H). IR: ν 1663, 3400 cm⁻¹. Anal. Calcd. for C₂₀H₂₂Cl₂N₄O: C, 59.27%; H, 5.47%; N, 13.82%. Found: C, 59.01%; H, 5.41%; N, 13.73%.

5.1.1.17. 1-(2,4-Dichlorophenyl)-N-(3,3-dimethylbutyl)-4-methyl-5-(1H-pyrrol-1-yl)-1H-pyrazole-3-carboxamide (**24**). Yield 97% as a white solid, mp 154–156 °C (from ethanol). ¹H NMR (CDCl₃): δ 0.97 (s, 9H), 1.52–1.57 (m, 2H), 2.32 (s, 3H), 3.43–3.49 (m, 2H), 6.21–6.22 (m, 2H), 6.58–6.59 (m, 2H), 6.88 (broad s, 1H, disappeared on treatment with D₂O), 7.21 (d, *J* = 8.8 Hz, 1H), 7.29 (dd, *J* = 8.5 and 2.2 Hz, 1H), 7.49 ppm (d, *J* = 2.2 Hz, 1H). IR: ν 1676, 3393 cm⁻¹. Anal. Calcd. for C₂₁H₂₄Cl₂N₄O: C, 60.15%; H, 5.77%; N, 13.36%. Found: C, 59.98%; H, 5.73%; N, 13.27%.

5.1.1.18. 1-(2,4-Dichlorophenyl)-4-methyl-N-(octan-2-yl)-5-(1H-pyrrol-1-yl)-1H-pyrazole-3-carboxamide (**25**). Yield 70% as a colorless oil. ¹H NMR (CDCl₃): δ 0.88 (t, *J* = 6.7 Hz, 3H), 1.24 (d, *J* = 6.6 Hz, 3H), 1.27–1.33 (m, 9H), 1.40–1.57 (m, 1H), 2.32 (s, 3H), 4.13–4.20 (m, 1H), 6.20–6.22 (m, 2H), 6.58–6.59 (m, 2H), 6.73 (broad s, 1H, disappeared on treatment with D₂O), 7.24 (d, *J* = 8.8 Hz, 1H), 7.30 (dd, *J* = 8.5 and 2.2 Hz, 1H), 7.48 ppm (d, *J* = 1.9 Hz, 1H). IR: ν 1667, 3408 cm⁻¹. Anal. Calcd. for C₂₃H₂₈Cl₂N₄O: C, 61.74%; H, 6.31%; N, 12.52%. Found: C, 61.65%; H, 6.27%; N, 12.46%.

5.1.1.19. 1-(2,4-Dichlorophenyl)-5-(2,5-dimethyl-1H-pyrrol-1-yl)-N-isopropyl-4-methyl-1H-pyrazole-3-carboxamide (**26**). Yield 97% as a white solid, mp 114–116 °C (from ethanol). ¹H NMR (CDCl₃): δ 1.29 (d, *J* = 6.6 Hz, 6H), 1.96 (s, 6H), 2.20 (s, 3H), 4.26–4.34 (m, 1H), 5.82 (s, 2H), 6.81 (broad s, 1H, disappeared on treatment with D₂O), 6.92 (d, *J* = 8.5 Hz, 1H), 7.20 (dd, *J* = 8.5 and 3.3 Hz, 1H), 7.53 ppm (d, *J* = 2.1 Hz, 1H). IR: ν 1649, 3327 cm⁻¹. Anal. Calcd. for C₂₀H₂₂Cl₂N₄O: C, 59.27%; H, 5.47%; N, 13.82%. Found: C, 59.09%; H, 5.41%; N, 13.71%.

5.1.1.20. N-tert-Butyl-1-(2,4-dichlorophenyl)-5-(2,5-dimethyl-1H-pyrrol-1-yl)-4-methyl-1H-pyrazole-3-carboxamide (**27**). Yield 98% as a white solid, mp 126–128 °C (from ethanol). ¹H NMR (CDCl₃): δ 1.51 (s, 9H), 1.96 (s, 6H), 2.19 (s, 3H), 5.81 (s, 2H), 6.90 (broad s, 1H, disappeared on treatment with D₂O), 6.91 (d, *J* = 8.5 Hz, 1H), 7.20 (dd, *J* = 8.5 and 2.3 Hz, 1H), 7.52 ppm (d, *J* = 2.3 Hz, 1H). IR: ν 1676, 3410 cm⁻¹. Anal. Calcd. for C₂₁H₂₄Cl₂N₄O: C, 60.15%; H, 5.77%; N, 13.36%. Found: C, 59.99%; H, 5.73%; N, 13.29%.

5.1.1.21. 1-(2,4-Dichlorophenyl)-5-(2,5-dimethyl-1H-pyrrol-1-yl)-4-methyl-N-tert-pentyl-1H-pyrazole-3-carboxamide (**28**). Yield 98% as a colorless oil. ¹H NMR (CDCl₃): δ 0.95 (t, *J* = 7.5 Hz, 3H), 1.45 (s, 6H), 1.86 (q, *J* = 7.5 Hz, 2H), 1.96 (s, 6H), 2.18 (s, 3H), 5.81 (s, 2H), 6.83 (broad s, 1H, disappeared on treatment with D₂O), 6.90 (d, *J* = 8.5 Hz, 1H), 7.20 (dd, *J* = 8.5 and 3.1 Hz, 1H), 7.52 ppm (d, *J* = 2.3 Hz, 1H). IR: ν 1672, 3406 cm⁻¹. Anal. Calcd. for C₂₂H₂₆Cl₂N₄O: C, 60.97%; H, 6.05%; N, 12.93%. Found: C, 60.71%; H, 6.01%; N, 12.80%.

5.1.1.22. 1-(2,4-Dichlorophenyl)-5-(2,5-dimethyl-1H-pyrrol-1-yl)-N-(3,3-dimethylbutyl)-4-methyl-1H-pyrazole-3-carboxamide (**29**). Yield 82% as a white solid, mp 143–145 °C (from ethanol). ¹H NMR (CDCl₃): δ 0.99 (s, 9H), 1.54–1.58 (m, 2H), 1.96 (s, 6H), 2.20 (s, 3H), 3.46–3.51 (m, 2H), 5.82 (s, 2H), 6.90 (d, *J* = 8.5 Hz, 1H), 6.96 (broad s, 1H, disappeared on treatment with D₂O), 7.20 (dd, *J* = 8.5 and 2.3 Hz, 1H), 7.53 ppm (d, *J* = 3.1 Hz, 1H). IR: ν 1655, 3332 cm⁻¹. Anal. Calcd. for C₂₃H₂₈Cl₂N₄O: C, 61.74%; H, 6.31%; N, 12.52%. Found: C, 61.59%; H, 6.27%; N, 12.40%.

5.1.1.23. 1-(2,4-Dichlorophenyl)-5-(2,5-dimethyl-1H-pyrrol-1-yl)-4-methyl-N-(octan-2-yl)-1H-pyrazole-3-carboxamide (**30**). Yield 68%

as a white solid, mp 59–61 °C (from ethanol-water). ¹H NMR (CDCl₃): δ 0.88 (t, *J* = 6.7 Hz, 3H), 1.25 (d, *J* = 6.6 Hz, 3H), 1.27–1.35 (m, 9H), 1.54–1.58 (m, 1H), 1.96 (s, 6H), 2.20 (s, 3H), 4.14–4.21 (m, 1H), 6.82 (s, 2H), 6.79 (broad s, 1H, disappeared on treatment with D₂O), 6.92 (d, *J* = 8.6 Hz, 1H), 7.20 (dd, *J* = 8.5 and 3.0 Hz, 1H), 7.53 ppm (d, *J* = 2.2 Hz, 1H). IR: ν 1671, 3408 cm⁻¹. Anal. Calcd. for C₂₅H₃₂Cl₂N₄O: C, 63.15%; H, 6.78%; N, 11.78%. Found: C, 62.79%; H, 6.74%; N, 11.66%.

5.1.1.24. 1-(2,4-Difluorophenyl)-5-(2,5-dimethyl-1H-pyrrol-1-yl)-N-(3,3-dimethylbutyl)-4-methyl-1H-pyrazole-3-carboxamide (**31**). Yield 89% as a white solid, mp 109–110 °C (from ethanol). ¹H NMR (CDCl₃): δ 0.99 (s, 9H), 1.55–1.59 (m, 2H), 1.91 (s, 6H), 2.19 (s, 3H), 3.45–3.48 (m, 2H), 5.82 (s, 2H), 6.87–6.94 (m, 3H), 7.11–7.17 ppm (m, 1H). IR: ν 3323, 1654 cm⁻¹. Anal. Calcd. for C₂₃H₂₈F₂N₄O: C, 66.65%; H, 6.81%; N, 13.52%. Found: C, 66.32%; H, 6.70%; N, 13.33%.

5.2. Molecular modeling

5.2.1. Computational chemistry

Molecular modeling and graphics manipulations were performed using the molecular operating environment (MOE) [17] and UCSF-CHIMERA software packages [18], running on a 2 CPU (PIV 2.0–3.0 GHz) Linux workstation. Energy minimizations and MD simulations were realized by employing the AMBER 9 [19] program selecting the Cornell force field [20].

5.2.2. Residue indexing

The convention used for the amino acid identifiers, according to the approach of Ballesteros and Weinstein [21] and van Rhee and Jacobson [22], facilitates comparison of aligned residues within the family of Group A GPCRs. The most conserved residue in a given TM (TM_X, where X is the TM number) is assigned the number X.50, and residues within a given TM are then indexed relative to the 50 position.

5.2.3. Docking simulations

The core structure of compound **29** was constructed using standard bond lengths and bond angles of the MOE fragment library. Geometry optimizations were accomplished with the MMFF94X force field, available within MOE. Docking simulations were carried out starting from the previously published inactive state of hCB₁ receptor model [9,10] which was built using the 2.8 Å crystal structure of bovine rhodopsin (PDB entry code 1F88) [23] as a structural template. Additional details regarding the receptor structure, site-directed mutagenesis data and methods applied in developing the hCB₁ receptor model are shown in Ref. [6] Compound **29** was docked into the energy-minimized receptor model by means of GOLD, 4.0 version, [24] a genetic algorithm-based software, taking the binding orientation of Rimobant in the hCB₁ bundle as a starting point. The region of interest used by GOLD was defined in order to contain the residues within 15 Å from the original position of Rimobant in the hCB₁ model [9]. The “allow early termination” option was deactivated while the remaining GOLD default parameters were used. The ligand was submitted to 100 genetic algorithm runs by selecting GOLD Score as a fitness function, without any other constraints. The best docked conformation for GOLD Score was then compared with the binding conformation of Rimobant in the hCB₁ bundle [9] and the root mean square deviation between the positions of the heavy atoms was calculated, this parameter being considered as a measure of the docking accuracy.

5.2.4. MD simulations

Refinement of the ligand/receptor complexes was achieved by in vacuo energy minimization with the SANDER module of AMBER,

applying an energy penalty force constant of $10 \text{ kcal mol}^{-1} \text{ \AA}^{-2}$ on the protein backbone atoms. The geometry-optimized complexes were then used as the starting point for subsequent 1 ns MD simulation, during which the protein backbone atoms were constrained by means of decreasing force constants; moreover, also the salt bridge between K3.28(192) and D6.58(366) as well as the H-bond between the ligand carboxamide oxygen and K3.28(192) were restrained. More specifically, an initial restraint with a force constant of $10 \text{ kcal mol}^{-1} \text{ \AA}^{-2}$ was applied on all the alpha carbons; this force constant decreased during the whole MD, and in the last 200 ps, its value was $0.01 \text{ kcal mol}^{-1} \text{ \AA}^{-2}$. As regards the intra-helix K3.28(192)/D6.58(366) H-bonds and the ligand/K3.28(192) interactions, a restraint of 10 and $50 \text{ kcal mol}^{-1} \text{ \AA}^{-2}$ were applied for 600 ps of MD simulation and, in the last 400 ps, the restraint was removed. General AMBER force field (GAFF) parameters were assigned to ligands, while the partial charges were calculated using the AM1-BCC method as implemented in the ANTECHAMBER suite of AMBER. A time step of 1 fs and a nonbonded pairlist updated every 25 fs were used for the MD simulations. The temperature was regulated by way of Langevin dynamics, with a collision frequency $\gamma = 1.0 \text{ ps}^{-1}$. An average structure was calculated from the last 100 ps trajectory and energy-minimized using the steepest descent and conjugate gradient methods as specified above. Root mean square (rms) deviations from the initial structures and interatomic distances were monitored using the PTRAJ module in AMBER.

5.3. CB_1 and CB_2 receptor binding assays

For both receptor binding assays, the new compounds were tested as previously described [11]. Binding affinities of reference compounds were evaluated in parallel with compounds **8–31**. K_i means concentration of the competing ligand that will bind to half the binding sites at equilibrium, in the absence of radioligand or other competitors. IC_{50} means concentration of competitor that competes for half of the specific binding (a measure of the competitor's potency at interacting with the receptor against the radioligand).

5.4. Pharmacological studies

The experimental procedure used here was in accordance with the Italian law on the 'Protection of animals used for experimental and other scientific reasons'.

5.4.1. Animals

Adult male Wistar rats (Charles River Laboratories, Calco, Italy), weighting approximately 500 g at the time of the tests, were used. Rats were individually housed in standard plastic cages with wood chip bedding. The animal facility was under an inverted 12:12 h light–dark cycle (lights on at 11:00 pm), at a constant temperature of $22 \pm 2 \text{ }^\circ\text{C}$ and relative humidity of approximately 60%. Rats were extensively habituated to handling and intraperitoneal injection. Food pellets (standard rat chow; Mucedola, Settimo Milanese, Italy) and water were available 24 h/day.

5.4.2. Experimental procedure

Two independent experiments were conducted, one testing compound **12** and the other testing compound **29**. On the test day of each experiment, rats were divided into four groups of $n = 7–8$, matched for body weight and food intake over the 3 days preceding the start of the experiment, and treated with 0, 0.1, 1, and 10 mg/kg compound **12** or 0, 3, and 10 mg/kg compound **29**. Compounds **12** or **29** were suspended in saline with a few drops of Tween 80 and administered intraperitoneally (injection volume: 3 mL/kg) 30 min before lights off. Food and water intake was recorded 60, 120, 180,

240, 300, 360, and 1440 min after lights off (1440 min correspond to 24 h) by weighing food pellets and bottles with a 0.1-g accuracy.

5.4.3. Statistical analysis

Data on the effect of compounds **12** or **29** on cumulative food and water intake over the first 360 min were analyzed by separate 2-way (treatment; time) ANOVAs with repeated measures on the factor 'time', followed by the Newman–Keuls test for post hoc comparisons. Data on the effect of compounds **12** or **29** on food and water intake at the 1440-min time interval were analyzed by separate 1-way ANOVAs, followed by the Newman–Keuls test for post hoc comparisons.

5.5. Pharmacokinetics

Pharmacokinetics and brain distribution studies were performed in Wistar rats (Charles River Laboratories, Calco, Italy). Animals were quarantined for approximately 1 week with an inverted day-night period prior the study. They were housed under standard conditions and had free access to water and standard laboratory rodent diet. Compound **12** or **29** was administered intraperitoneally at the dose of 10 mg/kg (formulation: 2% tween 80 and 98% saline at 1 mL/kg). Plasma and brains were collected from each rat ($n = 18$) at the following timepoints: 30, 60, 120, 240, 480 min and 24 h. Plasma and brain samples were kept frozen ($-80 \text{ }^\circ\text{C}$) until submission to extraction and LC-MS/MS analysis. Plasma samples ($100 \text{ }\mu\text{L}$) were spiked with $10 \text{ }\mu\text{L}$ of internal standard (IS) (100 ng/mL of compound **4**) and treated on a Sirocco filter plate (Waters) containing $400 \text{ }\mu\text{L}$ of a solution of 3% ammonia (3.2% in water) in MeOH. The plate was shaken for 20 min and the filtered samples ($350 \text{ }\mu\text{L}$) were analyzed by LC-MS/MS. Brain samples ($100 \text{ }\mu\text{L}$ of fresh brain homogenate made with 20 mM ammonium formate solution) were spiked with $10 \text{ }\mu\text{L}$ of IS (100 ng/mL of **4**) and treated on a Sirocco filter plate (Waters) likewise the plasma samples. The filtered samples were analyzed by LC-MS/MS. Sample analysis was performed on an Agilent HPLC (column: Synergy fusion RP $20 \times 2 \text{ mm}$ $2.5 \text{ }\mu\text{m}$; eluent: water, acetonitrile with 0.1% HCOOH gradient from 2%B to 100%B in 1.7 min flow 0.6 mL/min ; injected volume $25 \text{ }\mu\text{L}$, T column $40 \text{ }^\circ\text{C}$) coupled with a CTC PAL sample organizer and interfaced to a triple quadrupole API2000 (Applied Biosystem, Ontario, Canada). The mass spectrometer was operated using an APCI interface in positive mode (Gas1 60, Gas2 40, Source Temp. 450; NC 3). Three different Q1/Q3 transitions were applied 418.9/317.7 (DP 32, CE 30); 418.9/118.7 (DP 28, CE 54); 418.9/253.5 (DP 23, CE 59); Internal Standard. 520.7/158.6. Area of the samples was interpolated on 9 points calibration curves from 250 pg/mL (LLQ) to 100 ng/mL in brain and on a 10 points calibration curve from 500 pg/mL (LLQ) to 250 ng/mL in plasma. Pharmacokinetic parameters were calculated by a non-compartmental method using WinNolin 5.1 software (Pharsight, Mountain View, USA).

References

- [1] J.R. Sowers, Obesity as a cardiovascular risk factor, *Am. J. Med.* 115 (2003) 375–415.
- [2] (a) W.Y. Leung, T.G. Neil, J.C. Chan, B. Tomlinson, Weight management and current options in pharmacotherapy: orlistat and sibutramine, *Clin. Therapeut.* 25 (2003) 58–80; (b) European Medicines Agency recently decided to withdraw sibutramine due to cardiovascular risks.
- [3] J. Lee, K.-S. Song, J. Kang, S.H. Lee, J. Lee, New trends in medicinal chemistry approaches to antiobesity therapy, *Curr. Top. Med. Chem.* 9 (2009) 564–596.
- [4] (a) V. Di Marzo, Targeting the endocannabinoid system: to enhance or reduce? *Nat. Rev. Drug Discov.* 7 (2008) 438–455; (b) S. Pavlopoulos, G.A. Thakur, S.P. Nikas, A. Makriyannis, Cannabinoid receptors as therapeutic targets, *Curr. Pharm. Des* 12 (2006) 1751–1769; (c) L. Bellocchio, G. Mancini, V. Vicennati, R. Pasquali, U. Pagotto, Cannabinoid

- receptors as therapeutic targets for obesity and metabolic diseases, *Curr. Opin. Pharm.* 6 (2006) 586–591;
- (d) D.M. Lambert, C.J. Fowler, The endocannabinoid system: drug targets, lead compounds, and potential therapeutic applications, *J. Med. Chem.* 48 (2005) 5059–5087.
- [5] (a) R.S. Padwal, S.R. Majumdar, Drug treatments for obesity: orlistat, sibutramine, and rimonabant, *Lancet* 369 (2007) 71–77;
- (b) S.A. Doggrel, Is rimonabant efficacious and safe in the treatment of obesity? *Expert Opin. Pharmacother.* 9 (2008) 2727–2731;
- (c) D.R. Janero, A. Makriyannis, Cannabinoid receptor antagonists: pharmacological opportunities, clinical experience, and translational prognosis, *Expert Opin. Drug Disc.* 14 (2009) 43–65.
- [6] (a) H.J. Seo, M.J. Kim, S.H. Lee, S.-H. Lee, M.E. Jung, M.-S. Kim, K. Ahn, J. Kim, J. Lee, Synthesis and structure-activity relationship of 1,2,4-triazole-containing diarylpyrazolyl carboxamide as CB1 cannabinoid receptor-ligand, *Bioorg. Med. Chem.* 18 (2010) 1149–1162;
- (b) M. Cooper, J.-M. Receveur, E. Bjurling, P.K. Nørregaard, P.A. Nielsen, N. Sköld, T. Högberg, Exploring SAR features in diverse library of 4-cyano-methyl-pyrazole-3-carboxamides suitable for further elaborations as CB1 antagonists, *Bioorg. Med. Chem. Lett.* 20 (2010) 26–30;
- (c) J. Boström, R.I. Olsson, J. Tholander, P.J. Greasley, E. Ryberg, H. Nordberg, S. Hjorth, L. Cheng, Novel thioamide derivatives as neutral CB1 receptor antagonists, *Bioorg. Med. Chem. Lett.* 20 (2010) 479–482;
- (d) J.S. Debenham, C.B. Madsen-Duggan, R.B. Toupence, T.F. Walsh, J. Wang, X. Tong, S. Kumar, J. Lao, T.M. Fong, J.C. Xiao, C.R.-R.C. Huang, C.-P. Shen, Y. Feng, D.J. Marsh, D.S. Stribling, L.P. Shearman, A.M. Strack, M.T. Goulet, Furo [2,3-*b*]pyridine-based cannabinoid-1 receptor inverse agonists: synthesis and biological evaluation. Part 1, *Bioorg. Med. Chem. Lett.* 20 (2010) 1448–1452;
- (e) J.H.M. Lange, H.K.A.C. Coolen, M.A.W. van der Neut, A.J.M. Borst, B. Stork, P.C. Vermeer, C.G. Kruse, Design, synthesis, biological properties, and molecular modeling investigations of novel tacrine derivatives with a combination of acetylcholinesterase inhibition and cannabinoid CB1 receptor antagonism, *J. Med. Chem.* 53 (2010) 1338–1346;
- (f) H. Pettersson, A. Bülow, F. Ek, J. Jensen, L.K. Ottesen, A. Fejzic, J.-N. Ma, A.L. Del Tredici, E.A. Currier, L.R. Gardell, A. Tabatabaei, D. Craig, K. McFarland, T.R. Ott, F. Piu, E.S. Burstein, R. Olsson, Synthesis and evaluation of dibenzothiazepines: a novel class of selective cannabinoid-1 receptor inverse agonists, *J. Med. Chem.* 52 (2009) 1975–1982;
- (g) P. Diaz, S.S. Phatak, J. Xu, F. Astruc-Diaz, C.N. Cavasotto, M. Naguib, 6-Methoxy-N-alkyl isatin acylhydrazones derivatives as a novel series of potent selective cannabinoid receptor 2 inverse agonists: design, synthesis, and binding mode prediction, *J. Med. Chem.* 52 (2009) 433–444;
- (h) G. Szabó, B. Varga, D. Páyer-Lengyel, A. Szemző, P. Erdélyi, K. Vukics, J. Szikra, E. Hegyi, M. Vastag, B. Kiss, J. Laszy, I. Gyertyán, J. Fischer, Chemical and biological investigation of cyclopropyl containing diaryl-pyrazole-3-carboxamides as novel and potent cannabinoid type 1 receptor antagonists, *J. Med. Chem.* 52 (2009) 4329–4337.
- [7] Representative bioisosteres of 1 are depicted in our previous paper (see Ref. [9]).
- [8] (a) D.A. Griffith, J.R. Hadcock, S.C. Black, P.A. Iredale, P.A. Carpino, P. Da Silva-Jardine, R. Day, J. DiBrino, R.L. Dow, M.S. Landis, R.E. O'Connor, D.O. Scott, Discovery of 1-[9-(4-chlorophenyl)-8-(2-chlorophenyl)-9H-purin-6-yl]-4-ethyl-aminopiperidine-4-carboxylic acid amide hydrochloride (CP-945,598), a novel, potent, and selective cannabinoid type 1 receptor antagonist, *J. Med. Chem.* 52 (2009) 234–237;
- (b) R.L. Dow, P.A. Carpino, J.R. Hadcock, S.C. Black, P.A. Iredale, P. Da Silva-Jardine, S.R. Schneider, E.S. Paight, D.A. Griffith, D.O. Scott, R.E. O'Connor, C.I. Nduaka, Discovery of 2-(2-chlorophenyl)-3-(4-chlorophenyl)-7-(2,2-difluoropropyl)-6,7-dihydro-2H-pyrazolo[3,4-*f*][1,4]oxazepin-8(5H)-one (PF-514273), a novel, bicyclic lactam-based cannabinoid-1 receptor antagonist for the treatment of obesity, *J. Med. Chem.* 52 (2009) 2652–2655;
- (c) J.S. Debenham, C.B. Madsen-Duggan, J. Wang, X. Tong, J. Lao, T.M. Fong, M.-T. Schaeffer, J.C. Xiao, C.C.R.-R. Huang, C.-P. Shen, D.S. Stribling, L.P. Shearman, A.M. Strack, D.E. MacIntyre, J.J. Hale, T.F. Walsh, Pyridopyrimidine based cannabinoid-1 receptor inverse agonists: synthesis and biological evaluation, *Bioorg. Med. Chem. Lett.* 19 (2009) 2591–2594;
- (d) R. Smith, A.Z. Fathi, S.-E. Brown, S. Choi, J. Fan, S. Jenkins, H.C.E. Kluender, A. Konkar, R. Lavoie, R. Mays, J. Natoli, S.J. O'Connor, A.A. Ortiz, B. Podlogar, C. Taing, S. Tomlinson, T. Tritto, Z. Zhang, Constrained analogs of CB1 antagonists: 1,5,6,7-tetrahydro-4H-pyrrolo[3,2-*c*]pyridine-4-one derivatives, *Bioorg. Med. Chem. Lett.* 17 (2007) 673–678.
- [9] R. Silvestri, M.G. Cascio, G. La Regina, F. Piscitelli, A. Lavecchia, A. Brizzi, S. Pasquini, M. Botta, E. Novellino, V. Di Marzo, F. Corelli, Synthesis, cannabinoid receptor affinity, and molecular modeling studies of substituted 1-aryl-5-(1H-pyrrol-1-yl)-1H-pyrazole-3-carboxamides, *J. Med. Chem.* 51 (2008) 1560–1576.
- [10] R. Silvestri, A. Ligresti, G. La Regina, F. Piscitelli, A. Lavecchia, A. Brizzi, S. Pasquini, M. Allarà, N. Fantini, M.A.M. Carai, E. Novellino, G. Colombo, V. Di Marzo, F. Corelli, Synthesis, cannabinoid receptor affinity, molecular modeling studies and in vivo pharmacological evaluation of new substituted 1-aryl-5-(1H-pyrrol-1-yl)-1H-pyrazole-3-carboxamides. 2. Effect of the 3-carboxamide substituent on the affinity and selectivity profile, *Bioorg. Med. Chem.* 17 (2009) 5549–5564.
- [11] A. Brizzi, V. Brizzi, M.G. Cascio, T. Bisogno, R. Siriani, V. Di Marzo, Design, synthesis, and binding studies of new potent ligands of cannabinoid receptors, *J. Med. Chem.* 48 (2005) 7343–7350.
- [12] Y. Cheng, W.H. Prusoff, Relationship between the inhibition constant (K₁) and the concentration of inhibitor which causes 50 per cent inhibition (I₅₀) of an enzymatic reaction, *Biochem. Pharmacol.* 22 (1973) 3099–3108.
- [13] (a) D. Hurst, U. Umejiego, D. Lynch, H. Seltzman, S. Hyatt, M. Roche, S. McAllister, D. Fleischer, A. Kapur, M. Abood, S. Shi, J. Jones, D. Lewis, P. Reggio, Biarylpyrazole inverse agonists at the cannabinoid CB1 receptor: importance of the C-3 carboxamide oxygen/lysine3.28(192) interaction, *J. Med. Chem.* 49 (2006) 5969–5987;
- (b) D.P. Hurst, D.L. Lynch, J. Barnett-Norris, S.M. Hyatt, H.H. Seltzman, M. Zhong, Z.H. Song, J. Nie, D. Lewis, P.H. Reggio, N-(piperidin-1-yl)-5-(4-chlorophenyl)-1-(2,4-dichlorophenyl)-4-methyl-1H-pyrazole-3-carboxamide (SR141716A) interaction with LYS 3.28(192) is crucial for its inverse agonism at the cannabinoid CB1 receptor, *Mol. Pharmacol.* 62 (2002) 1274–1287.
- [14] S.D. McAllister, G. Rizvi, S. Anavi-Goffer, D.P. Hurst, J. Barnett-Norris, D.L. Lynch, P.H. Reggio, M.E. Abood, An aromatic microdomain at the cannabinoid CB(1) receptor constitutes an agonist/inverse agonist binding region, *J. Med. Chem.* 46 (2003) 5139–5152.
- [15] G. Colombo, R. Agabio, G. Diaz, C. Lobina, R. Reali, G.L. Gessa, Appetite suppression and weight loss after the cannabinoid antagonist SR 141716, *Life Sci.* 63 (1998) PL113–117.
- [16] V. Di Marzo, S.K. Goparaju, L. Wang, J. Liu, S. Bátkai, Z. Járαι, F. Fezza, G.I. Miura, R.D. Palmiter, T. Sugiura, G. Kunos, Leptin-regulated endocannabinoids are involved in maintaining food intake, *Nature* 410 (2001) 822–825.
- [17] Molecular Operating Environment (MOE), Version 2005.06. Chemical Computing Group, Inc, Montreal, Canada, 2005.
- [18] C.C. Huang, G.S. Couch, E.F. Pettersen, T.E. Ferrin, Chimera: an extensible molecular modelling application constructed using standard components, *Pac. Symp. Biocomput.* 1 (1996) 724.
- [19] D.A. Case, T.A. Darden, T.E. Cheatham III, C.L. Simmerling, J. Wang, R.E. Duke, R. Luo, K.M. Merz, D.A. Pearlman, M. Crowley, R.C. Walker, W. Zhang, B. Wang, S. Hayik, A. Roitberg, G. Seabra, K.F. Wong, F. Paesani, X. Wu, S. Brozell, V. Tsui, H. Gohlke, L. Yang, C. Tan, J. Mongan, V. Hornak, G. Cui, P. Beroza, D.H. Mathews, C. Schafmeister, W.S. Ross, P.A. Kollman, AMBER 9. University of California, San Francisco, 2006.
- [20] W.D. Cornell, P. Cieplak, C.I. Bayly, I.R. Gould, K.M. Merz Jr., D.M. Ferguson, D.C. Spellmeyer, T. Fox, J.W. Caldwell, P.A. Kollman, A second generation force field for the simulation of proteins, nucleic acids, and organic molecules, *J. Am. Chem. Soc.* 117 (1995) 5179–5197.
- [21] J.A. Ballesteros, H. Weinstein, Integrated methods for the construction of three-dimensional models and computational probing of structure-function relations in G-protein coupled receptors, *Methods Neurosci.* 25 (1995) 366–428.
- [22] A.M. van Rhee, K.A. Jacobson, Molecular architecture of G-protein-coupled receptors, *Drug Dev. Res.* 37 (1996) 1–38.
- [23] K. Palczewski, T. Kumasaka, T. Hori, C.A. Behnke, H. Motoshima, B.A. Fox, I.L. Trong, D.C. Teller, T. Okada, R.E. Stenkamp, M. Yamamoto, M. Miyano, Crystal structure of rhodopsin: a G protein-coupled receptor, *Science* 289 (2000) 739–745.
- [24] (a) GOLD, Version 4.0. CCDC Software Limited, Cambridge, U.K, 2008;
- (b) G. Jones, P. Willett, R.C. Glen, A.R. Leach, R. Taylor, Development and validation of a genetic algorithm for flexible docking, *J. Mol. Biol.* 267 (1997) 727–748.